OXFORD

Journal of Geophysics and Engineering

Journal of Geophysics and Engineering (2019) **16**, 926–938 doi:10.1093/jge/gxz056

Estimation of in situ anisotropy parameters from two perpendicular walkaway VSP lines in South Pars field

Mohammad Mahdi Abedi [1,3], **Mahtab Rashidi Fard** [2] **and Mohammad Ali Riahi** [1,*]

[1] Institute of Geophysics, University of Tehran, Tehran, Iran
[2] School of Mining Engineering, College of Engineering, University of Tehran, Tehran, Iran
[3] Norwegian University of Science and Technology, Department of Petroleum Engineering and Applied Geophysics, Trondheim, Norway

*Corresponding author: Mohammad Ali Riahi. E-mail: mariahi@ut.ac.ir

Received 25 July 2018, revised 17 May 2019
Accepted for publication 29 June 2019

Abstract

Vertical phase slowness and polarization angle are the in situ parameters of P-wave propagation that can be derived from walkaway vertical seismic profiling (VSP) data. To use these data for estimating anisotropy parameters, we obtain an explicit equation of vertical slowness as a function of polarization angle for P-wave propagation in transversely isotropic with vertical symmetry axis (VTI) media. We use this equation to estimate anisotropy parameters of a target layer in the South Pars field, Iran. This field is one of the world's largest gas fields. We show that the orthorhombic symmetry is a reasonable assumption for this layer, providing some geological and petrophysical information. Two walkaway VSP lines along the symmetry axes of the presumed orthorhombic layer are used to estimate its parameters. Seven is the maximum number of parameters that can be estimated using P-wave data in this acquisition pattern. Of those estimated parameters are six of the Tsvankin style parameters for orthorhombic media, plus an approximate combination of two others that define vertical S-wave splitting. We show that a previous method, which is based on weak anisotropy approximation, leads to considerable errors, even in models where the magnitude of anisotropy parameters do not exceed 0.1. We design a numerical experiment to study the reliability of the estimated parameters by the exact approach and show the importance of acquisition pattern in this regard. To show applicability, these parameters are used to estimate the in situ fracture properties of the studied layer.

Keywords: anisotropy, estimation, walkaway VSP, slowness, polarization

1. Introduction

Anisotropy is a scale-dependent concept. A material that is heterogeneous on small measurement scales can behave as homogeneous and anisotropic on larger scales. In seismic terms, this measurement scale is the wavelength. There is a considerable difference between the wavelength of surface seismic, log and laboratory measurements. Therefore, seismic anisotropy parameters should be measured by seismic data.

Walkaway VSP survey produces valuable data for estimating in situ anisotropy parameters around wellbores. In a typical walkaway VSP acquisition, several receivers are placed in a well at the depth interval of the target layer, and then a seismic source is used to generate shot records for different locations of that source. Different locations of the source provide wave propagation measurements at different polar and azimuthal angles. This information is necessary for the estimation of anisotropy parameters.

Local anisotropy parameters have been estimated using different methods by several authors (Miller and Spencer 1994; Miller *et al.* 1994; Horne and Leaney 2000; Zheng and Pšenčík 2002; Dewangan and Grechka 2003; Gomes *et al.* 2004; Grechka and Mateeva 2007; Grechka *et al.* 2007; Liu *et al.* 2014; Tamimi *et al.* 2015). They used slowness and polarization vectors to estimate local anisotropy using P-wave, or P- and SV-waves together. Wang (2011) used cross-hole P-wave data to estimate elliptical anisotropy parameters. Tsuji *et al.* 2011 estimated P-wave seismic anisotropy parameters using azimuthal normal moveout (NMO) velocity analysis and amplitude variation with azimuth, to reveal the stress state within the Kumano basin. Some methods, such as those of Zheng and Pšenčík (2002) and Gomes *et al.* (2004), use weak anisotropy approximation to make the equations simpler. Wang *et al.* (2019) develop an algorithm to obtain the fracture parameters from P-wave wide-azimuth surface seismic data. Their method uses weak anisotropy approximation too. Polarization angle was first considered as additional information for estimating local anisotropy parameters by Hsu *et al.* (1991) and de Parscau (1991). White *et al.* (1983) and Gaiser (1990) found interval phase velocities from horizontal and vertical phase slowness. Sun *et al.* (2009), estimated the anisotropic parameter based on the assumption of a transversely isotropic (TI) medium with vertical symmetry axis (VTI) or a TI medium with horizontal symmetry axis (HTI), and then confirmed their assumptions.

The reliability of slowness and slowness-polarization methods was assessed by Asgharzadeh *et al.* (2013) based on numerical experiments. They concluded that the selection of a proper method highly depends on the ability to accurately estimate horizontal slowness. Wherever laterally heterogeneous overburden layers are present, horizontal slowness cannot be estimated with reasonable accuracy. Grechka *et al.* (2019) developed a procedure to remove the influence of lateral heterogeneity on estimated anisotropy parameters when that heterogeneity is weak.

Tamimi *et al.* (2015) included S-waves in addition to P-waves in the slowness-polarization method for VTI. They showed that, depending on the data quality and coverage, SV-wave data provide useful information for estimating anisotropy parameters, especially near layer boundaries. However, VTI anisotropy assumption is too simplistic in most practical cases where we see azimuthal dependency of the parameters. Orthorhombic anisotropy can be the simplest realistic assumption for a symmetry system in many 3D geophysical problems (Bakulin *et al.* 2000b).

Bakulin *et al.* (2000a,b,c), studied fracture parameter estimation from surface seismic data and presented it in three parts based on types of anisotropic media; namely HTI, orthorhombic and monoclinic. They studied two models of fractured media that produce orthorhombic anisotropy, and derived fracture properties from anisotropy parameters for each model using weak anisotropy approximation. They also discussed several criteria to distinguish between these models.

The aim of this study is to estimate the in situ anisotropy parameters of a target layer in the South Pars field, Iran. South Pars field is one of the world's largest gas fields and is considered a significant source of energy for Iran. However, there are not many studies about anisotropy in different layers in this field.

In the following sections, we obtain an exact and explicit relation between the measurable P-wave propagation properties and VTI model properties. We explain how to use the data of two perpendicular walkaway VSP lines to estimate the possible anisotropy parameters, employing the proposed explicit relation. We design a numerical experiment to study the uncertainty of the estimated parameters. We present some complementary information to assume an anisotropy symmetry system for the studied layer. Finally, we use the parameters and the estimated anisotropy symmetry system to estimate presumed fracture properties.

2. Theory

2.1. Slowness-polarization relation in VTI media

The plane-wave solution of the wave equation in general anisotropic media results in the well-known Christoffel equation,

$$\left[G_{ik} - \rho v^2 \delta_{ik}\right] u_k = 0, \tag{1}$$

where v is the velocity along $\mathbf{n}$ (phase direction), u is the polarization vector, ρ is the density, $G_{ik} = c_{ijkl}\, n_j n_l$, is the Christoffel matrix that is dependent on the stiffness coefficients and the direction of the wave propagation, and δ_{ik} represents Kronecker's delta. This equation is a relation between the medium elastic properties, phase velocity and polarization vectors. For any phase direction, this equation yields three pairs of phase velocity and polarization vectors, and each corresponds to a wave mode. For inversion, this equation is used to estimate the medium stiffness properties having different measurements of phase velocity (or slowness) or polarization. However, by P-wave walkaway VSP data, the in situ measurements in this regard are vertical slowness and polarization angle. As shown in Appendix A, we obtain an explicit relation between the vertical phase slowness

(q) and polarization angle (ψ), for qP-wave propagation in VTI media as follows,

$$q^2(\psi) = \frac{(a_{55} - a_{11})^2 \tan\psi}{(a_{55} - a_{11})(a_{13} + a_{55})\, C + \left((a_{55} - a_{11})^2 a_{55} + a_{11} C^2\right) \tan\psi}, \tag{2}$$

where a_{ij} are the stiffness coefficients, normalized by the density of the medium, and

$$C = \sqrt{(a_{13} + a_{55})^2 \cot^2 2\psi + (a_{55} - a_{11})(a_{55} - a_{33})} - (a_{13} + a_{55}) \cot 2\psi. \tag{3}$$

We assume that the symmetry axis of the VTI medium matches the vertical well, where the q is measured. Using Thomsen (1986) notation for anisotropy parameters we obtain:

$$q^2(\psi) = \frac{1}{V_{P0}^2} \frac{(2\varepsilon + f)^2 \tan\psi}{C(2\varepsilon + f)\sqrt{f^2 + 2\delta f} + \left((1 + 2\varepsilon)^2 (1 - f) + C^2 (1 + 2\varepsilon)\right) \tan\psi}, \tag{4}$$

where δ and ε are anisotropy parameters, $f = 1 - V_{S0}^2/V_{P0}^2$, V_{P0} and V_{S0} are vertical P- and S-wave velocities, and C is defined as,

$$C = \sqrt{(f^2 + 2\delta f)\cot^2 2\psi + f^2 + 2\varepsilon f} - \sqrt{f^2 + 2\delta f} \cot 2\psi. \tag{5}$$

Having different measurements of q and ψ, equation (2) or (4) can be used in any nonlinear inversion procedure for estimating the model parameters. Equations (2) and (4) are derived as a solution of the Christoffel equation without making any simplifying assumption. These equations have four degrees of freedom but we can reduce them to two by fixing the two vertical parameters from well data. The new aspect of these exact equations compared to previous methods is their explicit form of vertical slowness as a function of polarization angle, which makes them more suitable for practical purposes such as inversion.

2.2. *Orthorhombic media*

In 3D models where the azimuthal variation of the wave propagation velocity is added to the vertical variations, it is necessary to decrease the degree of the presumed symmetry system for the medium. An orthorhombic model is characterized by three mutually orthogonal planes of symmetry. This model is a reasonable assumption for sedimentary environments where a combination of parallel vertical fractures with a VTI background medium creates an ideal orthorhombic symmetry.

P-wave propagation in elastic orthorhombic media is characterized by nine coefficients if the orientations of symmetry planes are known. While the estimation of all parameters needs multi-azimuthal measurements, seven coefficients can be determined from different measurements at two azimuths that match the vertical symmetry planes. This is because the Christoffel equation in the symmetry planes of orthorhombic media has the same form as in the TI models (Tsvankin 2012). Therefore, we can use equations (2) or (4) to obtain model parameters that affect P-wave kinematics and polarization at symmetry planes of an orthorhombic medium.

2.3. *Estimation of fracture parameters*

Schoenberg and Sayers (1995) studied extraction of fracture parameters from seismic data. In one case of an orthorhombic medium, the compliance matrix could be written as the sum of a background VTI and a HTI medium, based on linear slip theory (Schoenberg and Sayers 1995). As Schoenberg and Helbig (1997) explain, a stiffness tensor of a fracture-induced orthorhombic model can be estimated with eight independent parameters rather than nine. Three of these eight parameters are the dimensionless weakness of fractures that vary from zero to unity. Δ_V and Δ_H are tangential, and Δ_N denotes the normal fracture parameters. Based on one set of fractures in a plane parallel to the $[x_2, x_3]$ symmetry plane, fracture parameters are related to anisotropy parameters as follows (Bakulin *et al* 2000b):

$$\varepsilon^{(2)} - \varepsilon^{(1)} = 2f(f - 1)\Delta_N, \tag{6}$$

$$\delta^{(2)} - \delta^{(1)} = 2(f - 1)\left[(2f - 1)\Delta_N + \Delta_V\right], \tag{7}$$

where Δ_V is an estimation of fracture density and Δ_N is an indicator of fluids (Bakulin *et al.* 2000a). The only source of information about Δ_H is $\delta^{(3)}$.

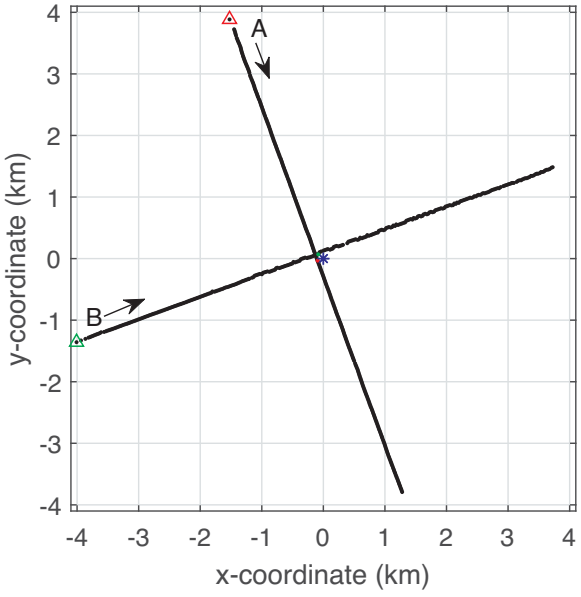

Figure 1. The acquisition map of the South Pars walkaway VSP lines, after moving the coordinate origin to the well location. Each black dot is a shot location. The star marks the well location. Two triangles indicate the left side in figures 2 and 3. In all figures, red indicates line A, and green indicates line B.

3. Anisotropy parameter estimation from field data

Data in this study belong to a walkaway VSP survey of a vertical well in the South Pars field, Iran. Shots were fired along two perpendicular acquisition lines (A and B), approximately crossing at the location of the well. Azimuthal directions of lines A and B are 160 and 70°, respectively. Each line is about 8 km long. The shot spacing on each line is about 25 m, and a three-component array seismic imager (ASI) receiver string with 15-m receiver interval is set up in the reservoir at the depth of the target layer. The middle geophone is at a depth of 2639 m.

Figure 1 shows the acquisition plan for both lines. Each black dot marks a shot location. The blue star marks the well location. The left to right direction of each line in figures 2 and 3 is also indicated in figure 1. Here and in all following figures, we indicate line A in red and line B in green.

Figure 2 shows the stacked sections of a surface seismic data under the acquisition lines (the stacked sections do not cover the entire VSP lines). This figure demonstrates that the assumption of a flat layer that is orthogonal to the receiver array (within the well) is reasonable. These assumptions are necessary for the application of the proposed $q(\psi)$ equations. Figure 3 shows two common receiver gather samples from both lines belonging to the first receiver in the five-receiver array. To use these data to invert for anisotropy parameters by equations (2) or (4), we need to obtain vertical slowness and polarization angles for each source-receiver pair.

One of the main advantages of the P-wave inversion in a walkaway VSP data is that only the first breaks are needed as input for the inversion procedure. The P-wave first arrivals are easily recognized; they have strong amplitudes and mainly no interference. We need traveltime to obtain the slowness, and the amplitudes of three component receivers to obtain the polarization angles. Figure 3 shows two examples of the travel times for P-wave direct arrivals obtained by an automatic tracking, interpolation and a slight smoothing. To convert the picked traveltimes to slowness, we use a three-point central difference method. Therefore, the five-receiver array allows us to perform the inversion at three consecutive depths. Figure 4 shows the converted vertical and horizontal slowness. By processing each VSP line separately, three distinct slowness surfaces are formed at corresponding depths.

To determine the P-wave polarization angle from vertical for each source to receiver pair, a Hodogram analysis is used. The input data of the Hodogram are amplitudes of three component receivers for a predefined window around the picked first arrivals. Figure 5 shows two Hodograms, one for horizontal components, and another for the vertical component versus the rotated horizontal component that is obtained from the first Hodogram.

After obtaining the $q-\psi$ data, we can use a $q(\psi)$ equation to estimate Thomsen's (1986) parameters for a VTI medium along each line. If the acquisition lines match the vertical symmetry planes of an orthorhombic medium, the estimated VTI parameters can be converted to Tsvankin's (1997) style orthorhombic parameters. Equation (4) is used in a

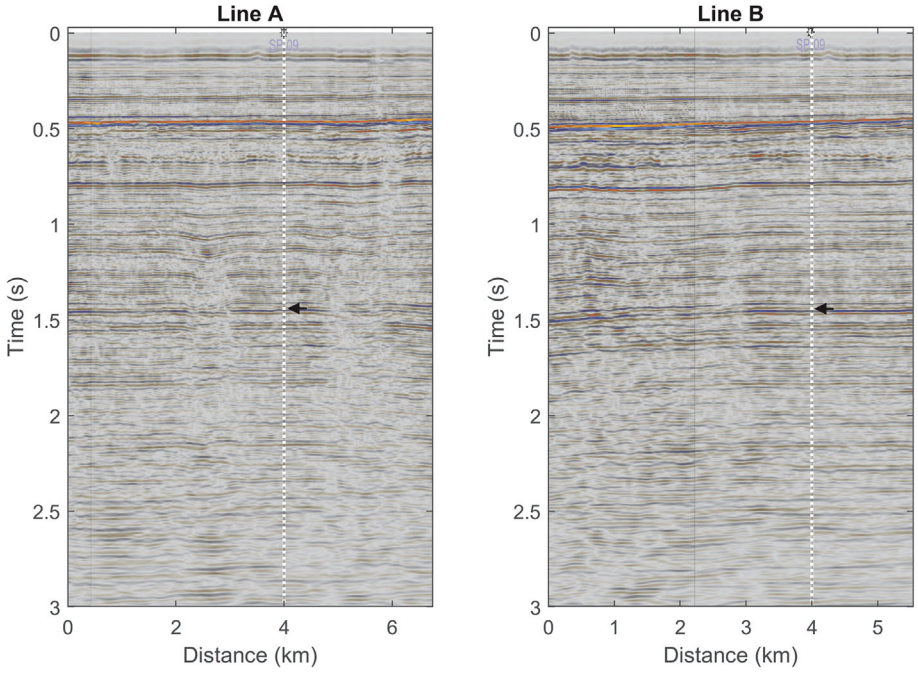

Figure 2. Stack sections of a surface seismic data along lines A and B. This shows that the studied area is not tectonically active and the target layer is mostly flat. The dotted white lines denote the well, and the arrows show the approximate location of the ASI tool.

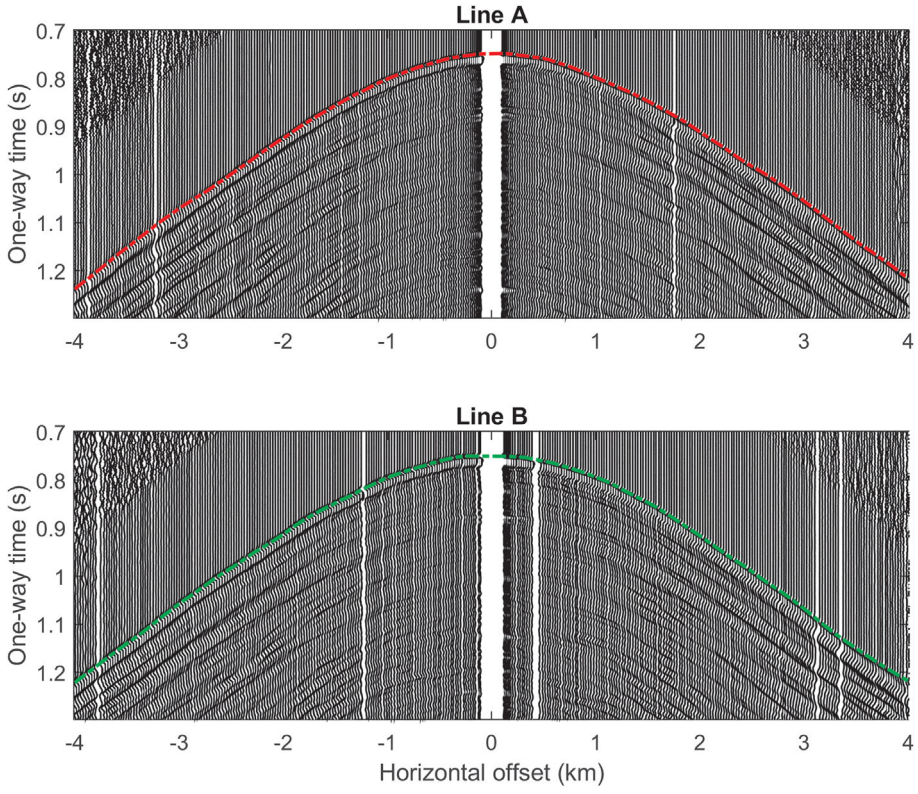

Figure 3. Two common receiver gather samples from Line A and Line B. P-wave first arrivals are plotted as the colored dashed lines.

trust-region-reflective least-squares inversion method to estimate anisotropy parameters along each line. This method is one of the optimization methods for solving nonlinear problems (More and Sorensen 1983; Byrd *et al.* 1988). Using the linear method of Miller and Spencer (1994) for the data in figure 4, the initial guess for the trust-region-reflective method is found. The scan ranges of parameters are determined as $\varepsilon \in [-0.2, 0.4]$, $\delta \in [-0.3, 0.3]$, $V_{P0} \in [2, 5]$ km/s. In this method, the optimum parameters are estimated in a way that the sum of square of differences between the estimated and observed

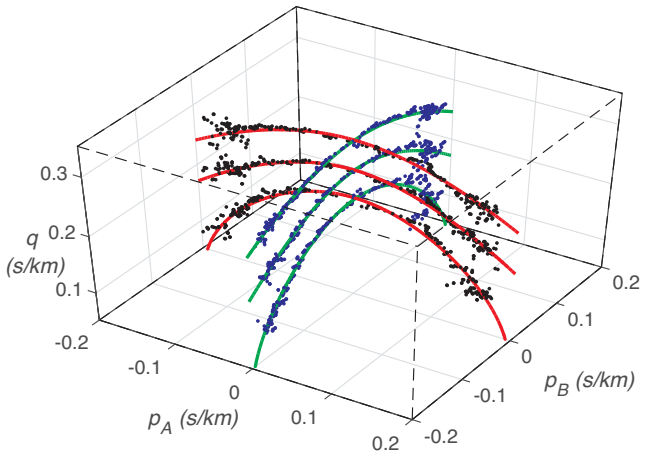

Figure 4. Vertical slowness versus horizontal slowness along both lines, converted from P-wave first breaks using a three point central difference at three consecutive depths.

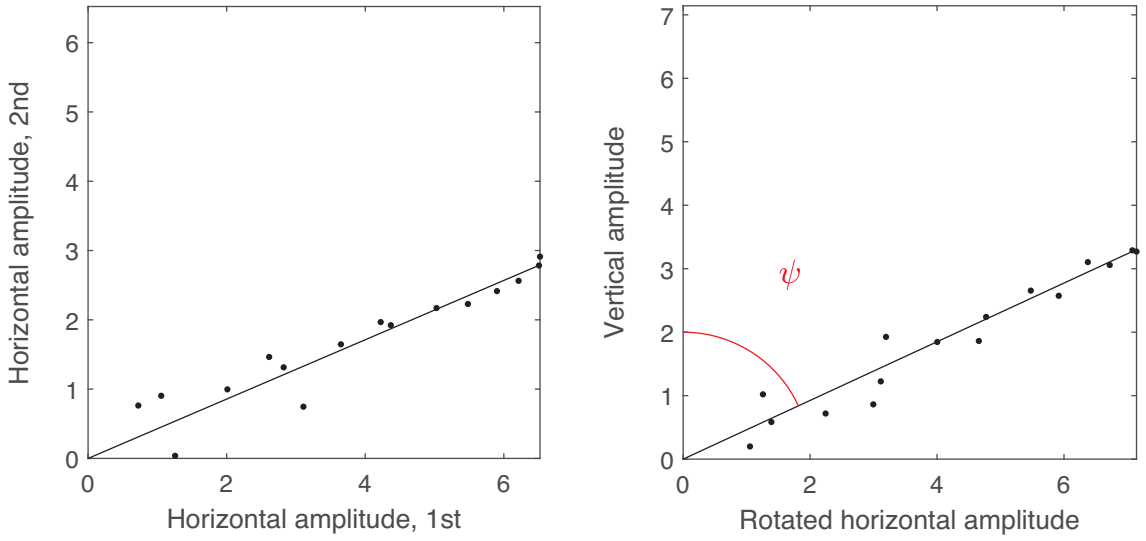

Figure 5. Hodogram analysis for estimation of polarization angle. The left-hand Hodogram represents horizontal components, while the right-hand one shows the vertical versus the rotated horizontal component. The dots show the sample amplitudes in a window around the picked first breaks.

slowness data is minimized. In figure 6, the slowness-polarization $(q - \psi)$ data points and the best fit of equation (4) are plotted and the inversion is illustrated. Here, the velocity ratio (V_{S0}/V_{P0}) is computed using the Dipole Sonic Imager (DSI) log. The estimated anisotropy coefficients and model parameters are shown in figure 6. As figure 6 indicates, the anisotropy parameters are close and non-zero along each acquisition line, indicating that the studied area is anisotropic in both directions. As both anisotropy parameters vary along two directions, the target layer can be characterized as an orthorhombic medium.

For comparison, a weak anisotropy approximation of Grechka and Mateeva (2007) is also plotted in each part of figure 6 using the estimated model parameters. In figure 6a and b, the weak anisotropy approximation is significantly erroneous, while it still has noticeable errors in figure 6c and d where the magnitude of anisotropy parameters is less than 0.1.

Next, all of the receivers are included in a single group and the average anisotropy parameters are determined over the entire depth interval of the ASI tool. We use a five-point stencil finite difference to obtain q from all five receivers, and average the polarization angles at three depths. The parameter f is also estimated using a limited range around the DSI log result. Figure 7 shows the converted $q - \psi$ data and the estimated VTI parameters along both lines. The weak anisotropy approximation of Grechka and Mateeva (2007) is also plotted for comparison.

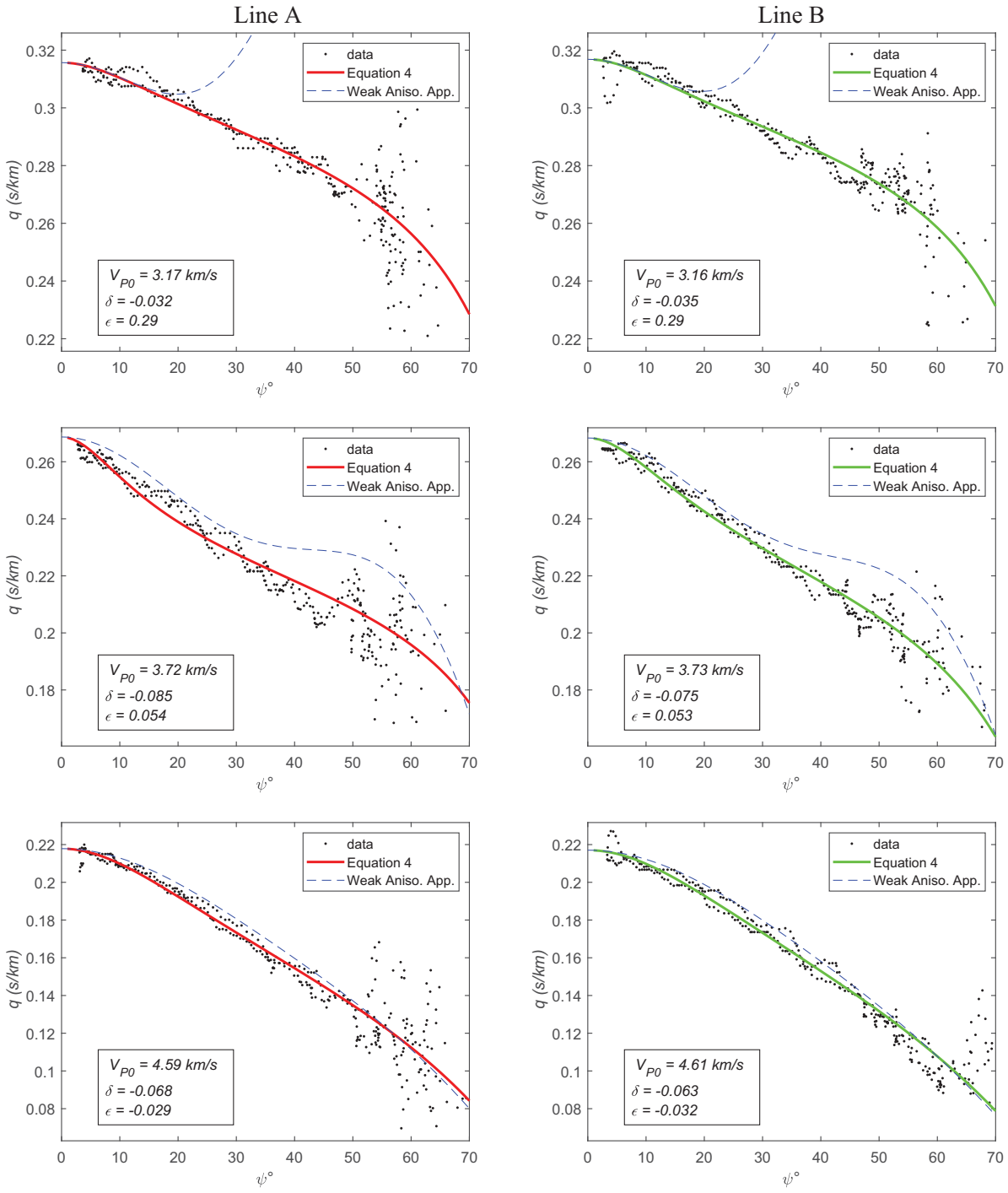

Figure 6. Slowness-polarization data (black dots) and the best fit of the presented equation (the red and green lines). The left column shows three consecutive depths along line A, and the right column shows the same depths along line B, respectively. The estimated model parameters using equation (4) are presented in each part. Using the estimated parameters, the approximation of Grechka and Mateeva (2007) is also plotted as the dashed lines.

3.1. Reliability of the estimated parameters

We design a numerical experiment to study the uncertainty of the estimated parameters by the aforementioned approach, and show the effect of an ideal acquisition pattern on that reliability. We calculate phase direction vectors for each ray traveling along each source to receiver path. We calculate n_1 and n_3, the horizontal and vertical components of phase direction, using $\frac{n_1}{n_3} = \frac{p}{q}$ where p and q are horizontal and vertical components of the slowness (figure 4). Note that $n_3 = \sqrt{1 - n_1^2}$. We can calculate q at the receiver location in depth, but p is calculated at surface; therefore, to estimate the phase directions in this

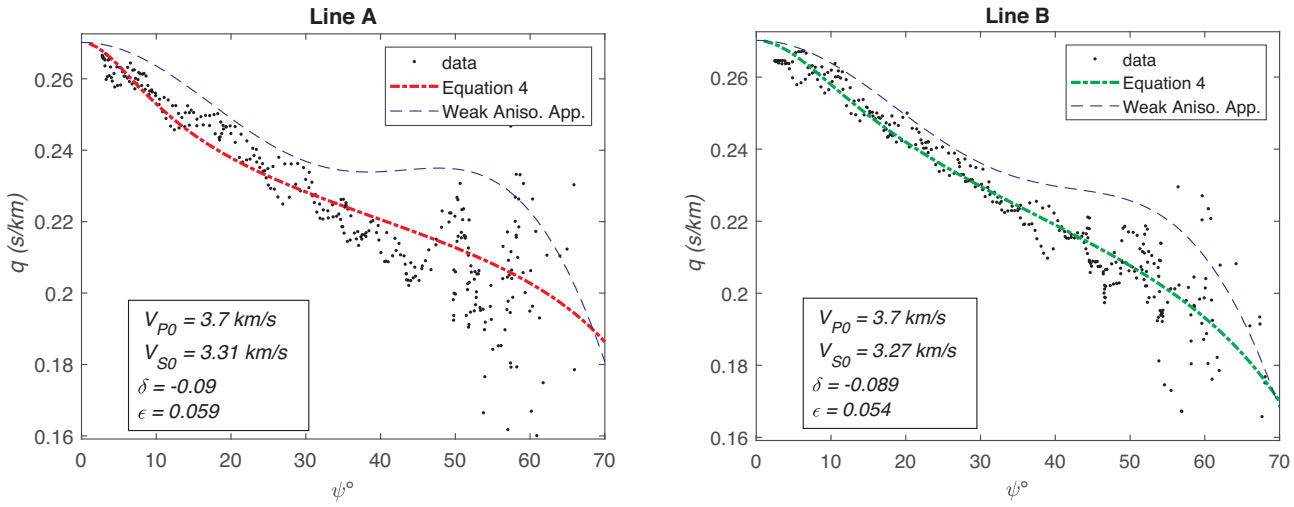

Figure 7. Estimation of anisotropy coefficients, using a five-point central difference stencil to obtain slowness and equation (4) to invert for model parameters. The weak anisotropy approximation is also plotted.

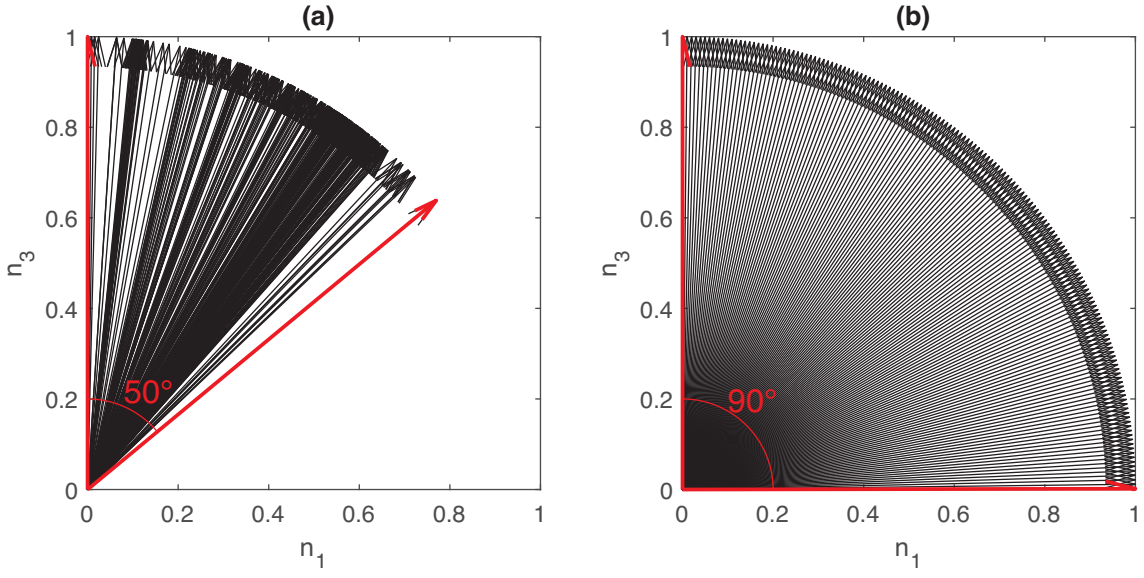

Figure 8. (a) Estimated phase directions at the location of the second receiver in line A; they are distributed unevenly while the maximum phase angle is 50°. (b) Ideal phase directions coverage, by the same number of arrows in part a (every second direction is plotted).

experiment, we assume that ray-parameter remains constant for each ray. Figure 8a shows the estimated phase directions for the second receiver in line A. The 319 arrows are distributed unevenly while the maximum coverage angle is 50°. Figure 8b shows an evenly distributed phase coverage for the same model.

We use the calculated phase directions (figure 8a), and the estimated parameters in the previous section (figure 7a), to model polarization and slowness vectors, shown as red dots in figure 9a. From figure 9a, the polarization angles are from 0 to 75°, while the slowness range is from $0.64/V_{P0}$ to $1/V_{P0}$. Therefore, our real data have unevenly covered 83% of ψ, and 36% of q range. Then we add different levels of normally distributed random noise to each data point and use the contaminated result in a least-squares inversion for estimation of the anisotropy parameters. Figure 9 shows the error bars for 10% of noise. Figure 10 shows the absolute value of relative average errors and relative standard deviation of the estimated ϵ and δ parameters, after repeating the experiment for 150 realizations of random noise. Horizontal and vertical axes show the standard deviation of the added random noise to each parameter as a percentage. It can be seen that a noisy polarization angle has a more destructive effect on the result than a noisy vertical slowness.

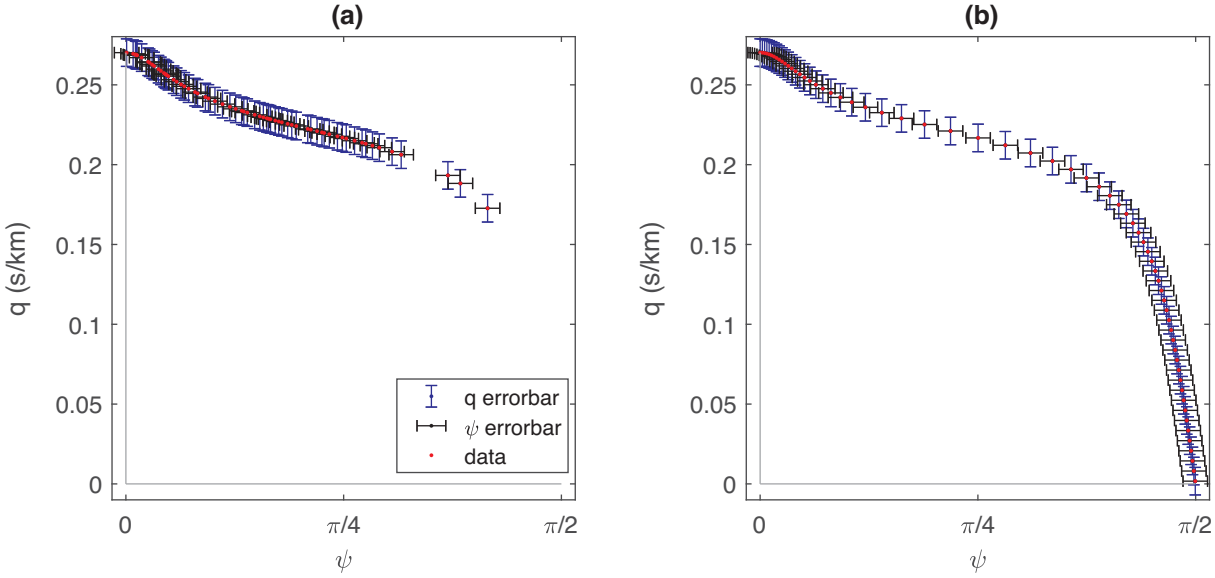

Figure 9. Modeled q-ψ data at phase direction in each part of figure 8. Error bars show the standard deviation of added random noise to both parameters. Every fifth data point is plotted for better illustration.

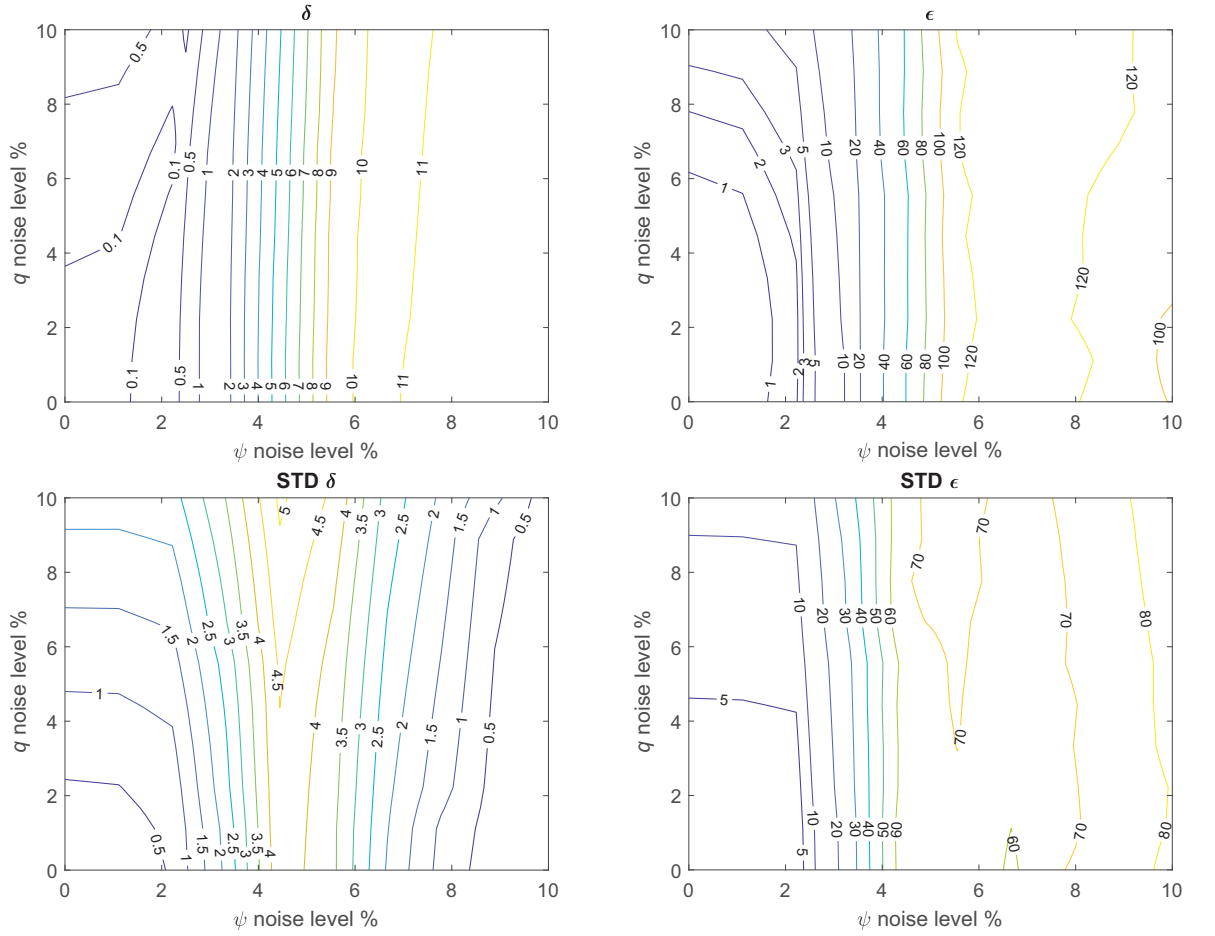

Figure 10. Reliability of the estimated anisotropy parameters. Upper row, average relative errors in estimated δ and ϵ as a function of different levels of a normal random noise added to the modeled polarization and slowness vectors. Lower row, relative standard deviation (STD) of the estimated parameters from noisy data, in percent.

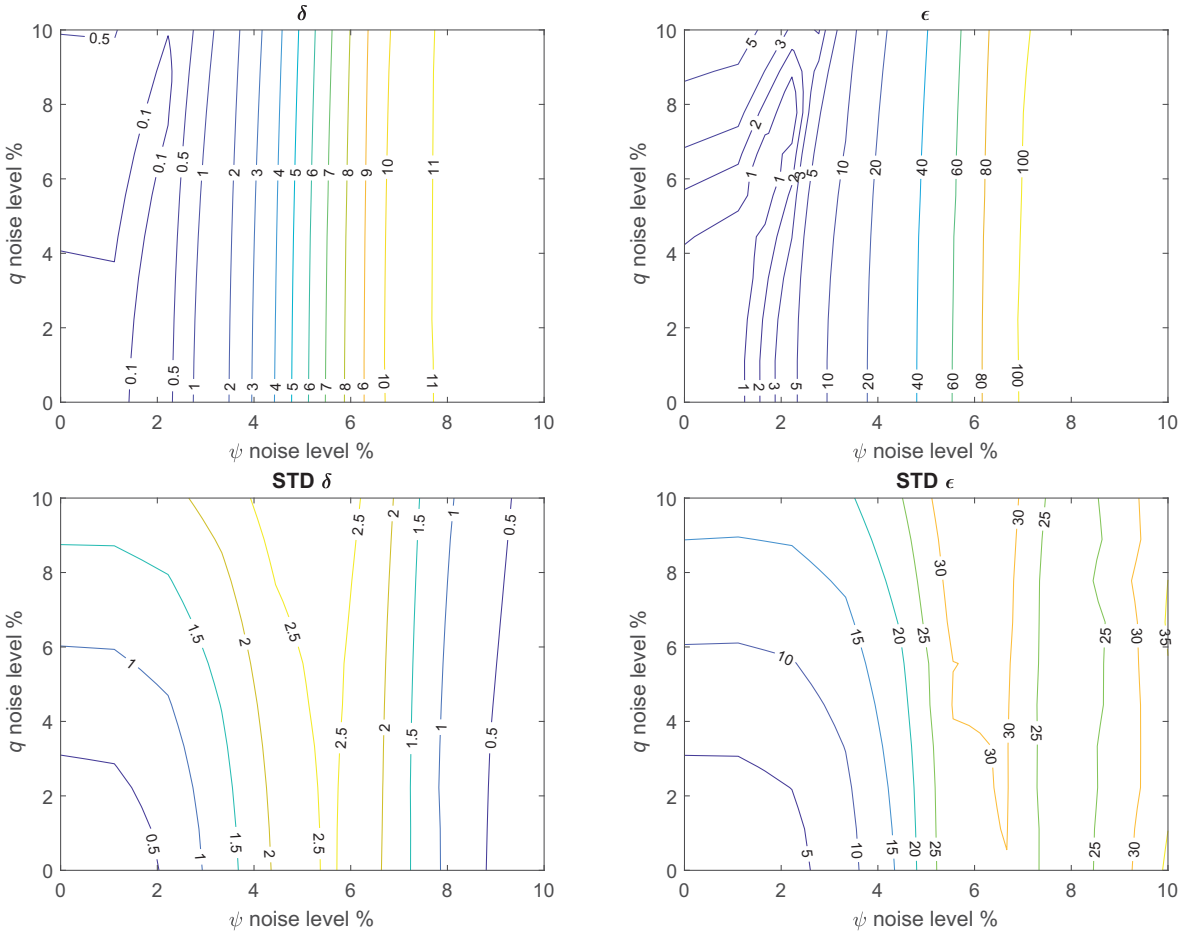

Figure 11. Reliability of estimated anisotropy parameters when using the ideal acquisition pattern that results in the full coverage in figure 10b. Upper row, average of relative errors in estimated δ and ϵ as a function of different levels of a normal random noise added to the modeled polarization and slowness vectors, in percent. Lower row, relative standard deviation (STD) of the estimated parameters from noisy data, in percent.

Next, we study the effect of acquisition pattern on the robustness of anisotropy parameter estimation. An ideal acquisition pattern would result in a uniform coverage of phase directions, from vertical to horizontal (figure 8b). Using the phase direction in figure 8b, we repeat the previous experiment keeping any other affecting parameters unchanged. Average values of data points in figure 9b are used to define the relative standard deviation of the added noise for both experiments. Figure 11 shows that a more suitable acquisition will increase the reliability of anisotropic parameters inversion for both parameters ϵ and δ. The improvement is more pronounced for higher degrees of noise in the polarization angle.

3.2. *Orthorhombic medium and fracture parameter calculation*

We have estimated and tested the VTI parameters along both lines. However, to relate these data to an orthorhombic environment and to use them for the fracture properties estimation, we have to show that these lines are properly aligned with the symmetry axis of an orthorhombic system. Therefore, the Formation Micro Imager (FMI) and DSI logs are used to validate the main direction of stress. Figure 12a illustrates the direction of the maximum horizontal stress, which is determined using the DSI log. We use this because of the independence of the detection method to breakout locations. Breakouts and the resulting directions of the maximum and minimum horizontal stresses around the wellbore are illustrated in figure 12. The breakouts on the FMI logs are shown about the depth of the tool position (figure 12d).

Both DSI and FMI logs show the same direction for the maximum horizontal stress. The dominant direction of the minimum horizontal stress in the adjacent area is similar to figure 12. Additionally, based on the geological map of the area (figure 13), the dip of the target layer is almost zero within the studied area, which denotes mild regional tectonics in the South Pars field.

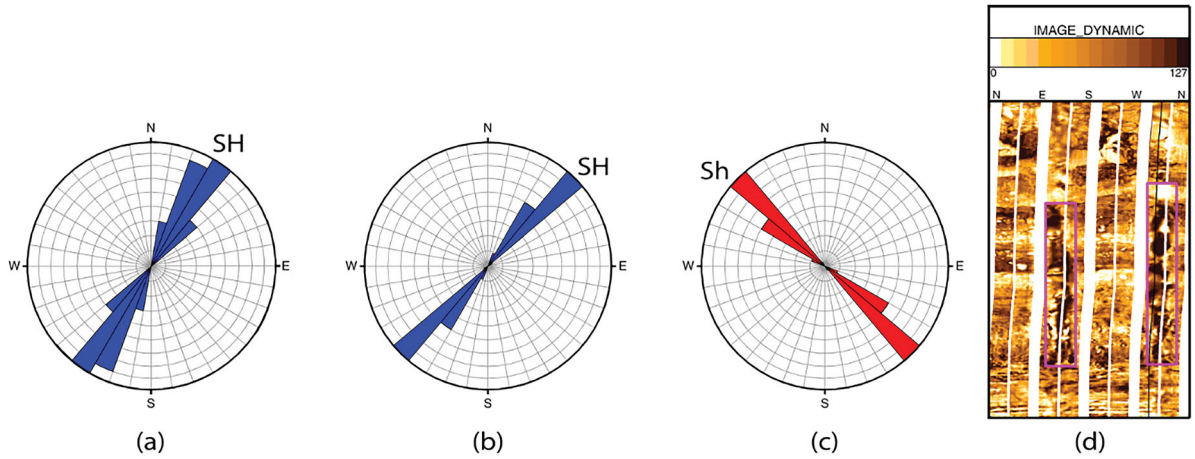

Figure 12. (a) The dominant direction of the maximum horizontal stress (SH) based on the DSI log. (b and c) The direction of the maximum and minimum horizontal stresses using the direction of breakouts. (d) Recognized breakouts in the image log (FMI). SH and Sh are the maximum and minimum horizontal stresses, respectively. The recognized breakouts are detected within the depth of receivers. These directions confirm the dominant direction of anisotropy in the studied area.

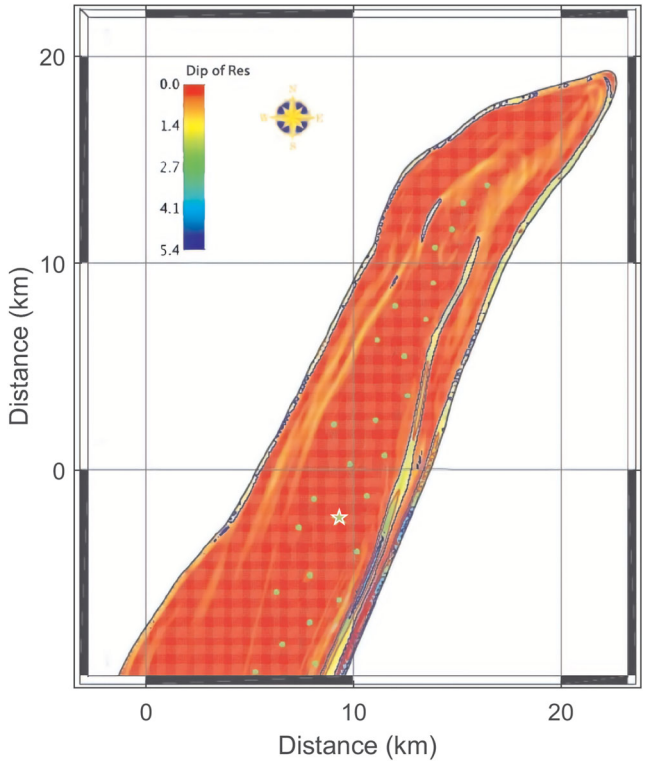

Figure 13. The dip map of the reservoir (field report). The white star shows the location of the studied well.

The evidence shows that the dominant direction of the regional fractures is in the NW-SE azimuthal direction. The differences between the anisotropy parameters along the VSP lines can be considered to be a result of the dominant direction of fractures, which is almost aligned with the acquisition line A.

Therefore, a flat orthorhombic assumption is reasonable for the target layer as a result of one system of vertical fractures in a VTI background. As the direction of the maximum and minimum stresses are aligned with the direction of the walkaway VSP lines, the estimated VTI parameters from these lines (figure 7) can be converted to orthorhombic parameters. We can estimate six of the Tsvankin (1997) style parameters for orthorhombic media, plus a combination of two other parameters that defines vertical S-wave splitting. The estimated orthorhombic parameters are: $V_{P0} = 3.7\,\text{km/s}$, $V_{S0} = 3.27\,\text{km/s}$, $\epsilon^{(1)} = 0.059$, $\epsilon^{(2)} = 0.054$, $\delta^{(1)} = -0.09$, $\delta^{(2)} = -0.089$, $\gamma^{(s)} \simeq 0.013$.

Now we use the estimated orthorhombic parameters in equations (6) to (7) to estimate the in situ fracture properties of the target layer. Taking line B direction labeled as (1) and line A labeled as (2), the tangential (Δ_V) and normal (Δ_N) fracture parameters are calculated to be 0.008 and 0.015, respectively. Since the parameter $\delta^{(3)}$ cannot be calculated from the two perpendicular walkaway VSP lines, and as no inclined reflector was detected in our case, we assume that fractures are rotationally invariant ($\Delta_V = \Delta_H$), and as a result, only one tangential weakness was determined.

The results demonstrate that by the slowness-polarization method it is possible to estimate anisotropy parameters that can be used to estimate intensity and fluid contents of mid-scale fractures. As any fracture parameter lies between zero and one, and based on our calculation of fracture parameters, crack density is not considerable in the studied area and the fluid content is insignificant.

4. Conclusion

Seismic anisotropy is a scale-dependent concept and its corresponding parameters should be estimated using seismic data. Walkaway VSP is a valuable acquisition pattern for anisotropy parameter estimation because it gives us information about vertical phase slowness and polarization angle at the depth of the target layer. To use the P-wave direct arrivals of such data for anisotropy parameter estimation, we obtained an explicit and exact $q(\psi)$ equation, dependent on model properties. We used the walkaway VSP data of two perpendicular lines in the South Pars field to estimate the anisotropy parameters of a target layer. We selected the trust-region-reflective inversion optimization methods, and designed a numerical experiment to study the validity of estimated anisotropy parameters. A study on the effect of proper coverage of slowness and polarization angles within their full range showed that a more suitable acquisition pattern will increase the reliability of anisotropic parameters inversion, for ε and δ anisotropy parameters. The complementary geological and petrophysical data of the studied area provide evidence for an orthorhombic symmetry assumption. Therefore, we estimated seven of the Tsvankin style parameters that govern P-wave propagation and shear wave splitting in orthorhombic media, and used them to estimate fracture properties.

Acknowledgements

The authors acknowledge the research council at University of Tehran. We acknowledge the journal reviewers, Nasser Tamimi, Alexey Stovas and two anonymous reviewers for their insightful comments. This research did not receive any specific grant from funding agencies.

Conflict of interest statement. None declared.

Appendix A. Christoffel equation in the slowness domain

Another form of the Christoffel equation (equation (1)) is written in the slowness domain. For VTI media it is written,

$$\begin{pmatrix} a_{11}p^2 + a_{55}q^2 - 1 & 0 & (a_{13} + a_{55})\,pq \\ 0 & a_{66}p^2 + a_{55}q^2 - 1 & 0 \\ (a_{13} + a_{55})\,pq & 0 & a_{55}p^2 + a_{33}q^2 - 1 \end{pmatrix} \begin{pmatrix} u_1 \\ u_2 \\ u_3 \end{pmatrix} = 0, \tag{A.1}$$

where p and q are the horizontal and vertical components of the phase slowness, and u_1, u_2, u_3 are the components of the polarization vector. For P-wave propagation, equation (A1) results in,

$$\begin{aligned} \left(a_{11}p^2 + a_{55}q^2 - 1\right)\sin\psi + (a_{13} + a_{55})\,pq\cos\psi = 0 \\ \left(a_{55}p^2 + a_{33}q^2 - 1\right)\cos\psi + (a_{13} + a_{55})\,pq\sin\psi = 0, \end{aligned} \tag{A.2}$$

where ψ is the vertical polarization angle. Dropping the parameter p in equations (A2), vertical slowness can be expressed as a function of polarization angle and stiffness coefficients (equation (2)), or Thomsen parameters (equation (4)).

References

Asgharzadeh, M., Bóna, A., Pevzner, R., Urosevic, M. & Gurevich, B., 2013. Reliability of the slowness and slowness-polarization methods for anisotropy estimation in VTI media from 3C walkaway VSP data, *Geophysics*, **78**, WC93–WC102.

Bakulin, A., Grechka, V. & Tsvankin, I., 2000a. Estimation of fracture parameters from reflection seismic data – Part II: Fractured models with orthorhombic symmetry, *Geophysics*, **65**, 1803–1817.

Bakulin, A., Grechka, V. & Tsvankin, I., 2000b. Estimation of fracture parameters from reflection seismic data – Part II: Fractured models with orthorhombic symmetry, *Geophysics*, **65**, 1803–1817.

Bakulin, A., Grechka, V. & Tsvankin, I., 2000c. Estimation of fracture parameters from reflection seismic data – Part III: Fractured models with monoclinic symmetry, *Geophysics*, **65**, 1818–1830.

Byrd, R.H., Schnabel, R.B. & Shultz, G.A., 1988. Approximate solution of the trust region problem by minimization over two-dimensional subspaces, *Mathematical Programming*, **40**, 247–263.

de Parscau, J., 1991. Relationship between phase velocities and polarization in transversely isotropic media, *Geophysics*, **56**, 1578–1583.

Dewangan, P. & Grechka, V., 2003. Inversion of multicomponent, multiazimuth, walkaway VSP data for the stiffness tensor, *Geophysics*, **68**, 1022–1031.

Gaiser, J.E., 1990. Transversely isotropic phase velocity analysis from slowness estimates, *Journal of Geophysical Research*, **95**, 241–254.

Gomes, E., Zheng, X., Pšenčík, I., Horne, S. & Leaney, S., 2004. Local determination of weak anisotropy parameters from walkaway VSP qP-wave data in the Java Sea region, *Studia Geophysica et Geodaetica*, **48**, 215–231.

Grechka, V. & Mateeva, A., 2007. Inversion of P-wave VSP data for local anisotropy: Theory and case study, *Geophysics*, **72**, D69–79.

Grechka, V., Mateeva, A., Gentry, C., Jorgensen, P., Lopez, J. & Franco, G., 2007. Estimation of seismic anisotropy from P-wave VSP data, *The Leading Edge*, **26**, 756–759.

Grechka, V., Tsvankin, I. & Contreras, P., 2019. Inversion of walkaway VSP data in the presence of lateral velocity heterogeneity, preprint arXiv:1901.02916.

Horne, S. & Leaney, S., 2000. Short note: Polarization and slowness component inversion for TI anisotropy, *Geophysical Prospecting*, **48**, 779–788.

Hsu, K., Schoenberg, M. & Walsh, J., 1991. Anisotropy from polarization and moveout, in *Proceedings of the 61st Annual International Meeting, SEG, Expanded Abstracts*, 1526–1529. Society of Exploration Geophysicists, Houston, Texas.

Liu, Y., Liang, X., Yin, X., Zhou, Y. & Li, Y., 2014. Estimation of Thomsen's anisotropic parameters from walkaway VSP and applications, *Applied Geophysics*, **11**, 23–30.

Miller, D.E., Leaney, S. & Borland, W.H., 1994. An in situ estimation of anisotropic elastic moduli for a submarine shale, *Journal of Geophysical Research*, **99**, 21659–21665.

Miller, D.E. & Spencer, C., 1994. An exact inversion for anisotropic moduli from phase slowness data, *Journal of Geophysical Research*, **99**, 21651–21657.

Moré, J.J. & Sorensen, D.C., 1983. Computing a trust region step, *SIAM Journal on Scientific and Statistical Computing*, **4**, 553–572.

Schoenberg, M. & Helbig, K., 1997. Orthorhombic media: Modeling elastic wave behavior in a vertically fractured earth, *Geophysics*, **62**, 1954–1974.

Schoenberg, M. & Sayers, C.M., 1995. Seismic anisotropy of fractured rock, *Geophysics*, **60**, 204–211.

Sun, X., Ling, Y., Gao, J., Sun, D. & Lin, J., 2009. Anisotropic parameter estimation based on 3D VSP and full azimuth seismic data, in *79th Annual International Meeting, SEG, Expanded Abstracts*, 4105–4109. Society of Exploration Geophysicists, Houston, Texas.

Tamimi, N., Tsvankin, I. & Davis, T.L., 2015. Estimation of VTI parameters using slowness-polarization inversion of P- and SV-waves, *Journal of Seismic Exploration*, **24**, 455–474.

Thomsen, L., 1986. Weak elastic anisotropy, *Geophysics*, **51**, 1954–1966,

Tsuji, T. et al. 2011. In situ stress state from walkaround VSP anisotropy in the Kumano basin southeast of the Kii Peninsula, Japan, *Geochemistry, Geophysics, Geosystems*, **12**, 1–18.

Tsvankin, I., 1997. Anisotropic parameters and P-wave velocity for orthorhombic media, *Geophysics*, **62**, 1292–1309.

Tsvankin, I., 2012. *Seismic Signatures and Analysis of Reflection Data in Anisotropic Media*, Society of Exploration Geophysicists, Houston, TX.

Wang, T., Yuan, S., Shi, P., Shuai, D., Luo, C. & Wang, S., 2019. AVAZ inversion for fracture weakness based on three-term Rüger equation, *Journal of Applied Geophysics*, **162**, 184–193.

Wang, Y., 2011. Seismic anisotropy estimated from P-wave arrival times in crosshole measurements, *Geophysical Journal International*, **184**, 1311–1316.

White, J.E., Martineau-Nicoletis, L. & Monash, C., 1983. Measured anisotropy in Pierre shale, *Geophysical Prospecting*, **31**, 709–725.

Zheng, X. & Pšenčík, I., 2002. Local determination of weak anisotropy parameters from qP-wave slowness and particle motion measurements, *Pure and Applied Geophysics*, **159**, 1881–1905.